J|A|C|S ARTICLES

Published on Web 06/08/2009

Photosynthetic Reaction Center Mimicry: Low Reorganization Energy Driven Charge Stabilization in Self-Assembled Cofacial Zinc Phthalocyanine Dimer−Fullerene Conjugate

Francis D'Souza,*,† Eranda Maligaspe,† Kei Ohkubo,‡ Melvin E. Zandler,† Navaneetha K. Subbaiyan,† and Shunichi Fukuzumi*,‡

Department of Chemistry, Wichita State University, 1845 Fairmount, Wichita, Kansas 67260-0051, and Department of Material and Life Science, Graduate School of Engineering, Osaka University, SORT, Japan Science and Technology Agency (JST), Suita, Osaka 565-0871, Japan

Received July 23, 2008; E-mail: francis.dsouza@wichita.edu; fukuzumi@chem.eng.osaka-u.ac.jp

Abstract: By employing well-defined self-assembly methods, a biomimetic bacterial photosynthetic reaction center complex has been constructed, and photoinduced electron transfer originating in this supramolecular donor−acceptor conjugate has been investigated. The biomimetic model of the bacterial "special pair" donor, a cofacial zinc phthalocyanine dimer, was formed via potassium ion induced dimerization of 4,5,4′,5′,4″, 5″,4‴,5‴-zinc tetrakis(1,4,7,10,13-pentaoxatridecamethylene)phthalocyanine. The dimer was subsequently self-assembled with functionalized fullerenes via "two-point" binding involving axial coordination and crown ether-alkyl ammonium cation complexation to form the donor−acceptor pair, mimicking the noncovalently bound entities of the bacterial photosynthetic reaction center. The adopted self-assembly methodology yielded a supramolecular complex of higher stability with defined geometry and orientation as revealed by the binding constant and computational optimized structure. Unlike the previously reported porphyrin analog, the present phthalocyanine macrocycle based model system exhibited superior electron-transfer properties including formation of a long-lived charge-separated state, a key step of the photosynthetic light energy conversion process. Detailed analysis of the kinetic data in light of the Marcus theory of electron transfer revealed that small reorganization energy of the relatively rigid phthalocyanine is primarily responsible for slower charge-recombination process. The importance of the cofacial dimer in stabilizing the charge-separated state is borne out in the present all-supramolecular "reaction center" donor−acceptor mimic.

Introduction

Structural studies of the photosynthetic reaction center of *R. viridis* and *R. sphaeroides* have revealed membrane-bound protein containing four bacteriochlorophylls, two bacteriopheophytins, and two quinones.[1] The primary electron donor, a "special pair" of two bacteriochlorophylls, is held apart noncovalently by about 3.2 Å with a slipped cofacial orientation. These reaction centers undergo sequential multistep electron transfer generating long-lived charge-separated states, a key feature needed for efficient harvesting of light energy.[1] A number of studies have reported on model compounds as photosynthetic reaction center mimics with an ultimate aim of harvesting solar energy by constructing photovoltaic devices.[2−7] There have also been a few studies mimicking the reaction centers of photosynthetic systems, by incorporation of a special pair into these models.[8−10] Although the self-assembly approach of building donor−acceptor pairs is more biomimetic, it has been difficult to control the distance and orientation because of

† Wichita State University.
‡ Osaka University.

(1) (a) Deisenhofer, J.; Epp, O.; Miki, K.; Huber, R.; Michel, H. *Nature* **1986**, *318*, 618–624. (b) Deisenhofer, J.; Michel, H. *Science* **1989**, *245*, 1463–1473. (c) Allen, P.; Feher, G.; Yeates, T. O.; Rees, D. C.; Deisenhofer, J.; Michel, H.; Huber, R. *Proc. Natl. Acad. Sci. U.S.A.* **1986**, *83*, 8589–8593. (d) Deisenhofer, J.; Epp, O.; Sinning, I.; Michel, H. *J. Mol. Biol.* **1995**, *246*, 429–457. (e) Jordan, P.; Fromme, P.; Witt, H.-T; Klukas, O.; Saenger, W.; Krauss, N. *Nature* **2001**, *411*, 909–917.

(2) (a) Wasielewski, M. R. *Chem. Rev.* **1992**, *92*, 435–461. (b) Connolly, J. S.; Bolton, J. R. In *Photoinduced Electron Transfer*; Fox, M. A., Chanon, M., Eds.; Elsevier: Amsterdam, 1988; Part D, pp 303−393. (c) Kurreck, H.; Huber, M. *Angew. Chem., Int. Ed. Engl.* **1995**, *34*, 849–866.

(3) (a) Gust, D.; Moore, T. A.; Moore, A. L. *Acc. Chem. Res.* **2001**, *34*, 40–48. (b) Gust, D.; Moore, T. A. In *The Porphyrin Handbook*; Kadish, K. M., Smith, K. M., Guilard, R., Eds.; Academic Press: Burlington, MA, 2000; Vol. 8, pp 153−190.

(4) (a) Martín, N.; Sánchez, L.; Illescas, B.; Pérez, I. *Chem. Rev.* **1998**, *98*, 2527–2548. (b) Diederich, F.; Gómez-López, M. *Chem. Soc. Rev.* **1999**, *28*, 263–277. (c) Guldi, D. M. *Chem. Commun.* **2000**, 321–327. (d) Guldi, D. M.; Prato, M. *Acc. Chem. Res.* **2000**, *33*, 695–703. (e) Guldi, D. M. *Chem. Soc. Rev.* **2002**, *31*, 22–36. (f) Balzani, V.; Credi, A.; Venturi, M. *ChemSusChem* **2008**, *1*, 26–58.

(5) (a) Meijer, M. E.; van Klink, G. P. M.; van Koten, G. *Coord. Chem. Rev.* **2002**, *230*, 141–163. (b) El-Khouly, M. E.; Ito, O.; Smith, P. M.; D'Souza, F. *J. Photochem. Photobiol. C* **2004**, *5*, 79–104. (c) Imahori, H.; Fukuzumi, S. *Adv. Funct. Mater.* **2004**, *14*, 525–536. (d) D'Souza, F.; Ito, O. *Coord. Chem. Rev.* **2005**, *249*, 1410–1422. (e) De la Escosura, A.; Martinez-Diaz, M. V.; Guldi, D. M.; Torres, T. *J. Am. Chem. Soc.* **2006**, *128*, 4112–4118. (f) Sanchez, L.; Martin, N.; Guldi, D. M. *Angew. Chem., Int. Ed.* **2005**, *44*, 5374–5382.

(6) (a) Fukuzumi, S. *Phys. Chem. Chem. Phys.* **2008**, *10*, 2283–2297. (b) Chitta, R.; D'Souza, F. *J. Mater. Chem.* **2008**, *18*, 1440–1471. (c) Fukuzumi, S.; Kojima, T. *J. Mater. Chem.* **2008**, *18*, 1427–1439. (d) Fukuzumi, S. *Eur. J. Inorg. Chem.* **2008**, 1351–1362.

weak interactions and the associated multiple equilibrium processes.[11−13] The majority of these studies utilized porphyrins as a light harvesting unit and an electron donor and fullerenes as an electron acceptor.[3−7] However, phthalocyanines (Pc's) have more attractive features as compared to porphyrins in view of their strong absorption in the 600−700 nm region, leading to a blue-coloring ability, which is accompanied by a robust nature and better electron donor ability (when appropriate substituents are present).[14] Despite the excellent light harvesting and electron donor properties of Pc's, supramolecular donor−acceptor ensembles of Pc's and fullerenes still remains challenging because of the synthetic difficulties associated in building host−guest assemblies. In addition, the low lying triplet excited state of Pc's, which is generally lower in energy than the charge-separated (CS) state of Pc-fullerene ensembles, has precluded attainment of the long-lived CS state.[15−20]

We report herein a biomimetic model of the bacterial special pair, that is, a supramolecular complex between a cofacial zinc phthalocyanine dimer obtained by complexation of the four crown ether units of phthalocyanine with potassium ions, and a fullerene functionalized with a pyridine coordinating entity and an alkyl ammonium cation entity for two point binding. Such potassium ion induced dimerization of 4,5,4′,5′,4″,5″,4‴,5‴-tetrakis(1,4,7,10,13-pentaoxa-tridecamethylene)phthalocyanine zinc(II), ZnTCPc, was first reported by Kobayashi and Lever.[21,22] As shown in Scheme 1, the potassium ion is sandwiched between two 15-crown-5 entities from two different phthalocyanines due to the size differences.[21,22] Next, the $K_4[ZnTCPc]_2$ dimer was allowed to interact with fullerene functionalized with a pyridine

(7) (a) Fukuzumi, S.; Guldi, D. M. In *Electron Transfer in Chemistry*; Balzani, V., Ed.; Wiley-VCH: Weinheim, 2001; Vol. 2, pp 270−337. (b) Fukuzumi, S. *Org. Biomol. Chem.* **2003**, *1*, 609–620. (c) Fukuzumi, S. *Bull. Chem. Soc. Jpn.* **2006**, *79*, 177–195. (d) Imahori, H.; Guldi, D. M.; Tamaki, K.; Yoshida, Y.; Luo, C.; Sakata, Y.; Fukuzumi, S. *J. Am. Chem. Soc.* **2001**, *123*, 6617–6628.

(8) (a) Sessler, J. L.; Johnson, M. R.; Lin, T.-Y.; Creager, S. E. *J. Am. Chem. Soc.* **1988**, *110*, 3659–3661. (b) Rodriguez, J.; Kirmaier, C.; Johnson, J. R.; Friesner, R. A.; Holten, D.; Sessler, J. L. *J. Am. Chem. Soc.* **1991**, *113*, 1652–1659. (c) Osuka, A.; Nakajima, S.; Maruyama, K.; Mataga, K.; Asahi, T.; Yamazaki, I.; Nishimura, Y.; Ohno, T.; Nozaki, K. *J. Am. Chem. Soc.* **1993**, *115*, 4577–4589. (d) Nakashima, S.; Taniguchi, S.; Okada, T.; Osuka, A.; Mizutani, Y.; Kitagawa, T. *J. Phys. Chem. A* **1999**, *103*, 9184–9189.

(9) (a) Ozeki, H.; Nomoto, A.; Ogawa, K.; Kobuke, Y.; Murakami, M.; Hosoda, K.; Ohtani, M.; Nakashima, S.; Miyasaka, H.; Okada, T. *Chem.−Eur. J.* **2004**, *10*, 6393–6401. (b) Isosomppi, M.; Tkachenko, N. V.; Efimov, A.; Lemmetyinen, H. *J. Phys. Chem. A* **2005**, *109*, 4881–4890.

(10) D'Souza, F.; Chitta, R.; Gadde, S.; Rogers, L. M.; Karr, P. A.; Zandler, M. E.; Sandanayaka, A. S. D.; Araki, Y.; Ito, O. *Chem.−Eur. J.* **2007**, *13*, 916–922.

(11) (a) Sessler, J. L.; Wang, B.; Springs, S. L.; Brown, C. T. In *Comprehensive Supramolecular Chemistry*; Atwood, J. L., Davies, J. E. D., MacNicol, D. D., Vögtle, F., Eds.; Pergamon: New York, 1996; Chapter 9. (b) Hayashi, T.; Ogoshi, H. *Chem. Soc. Rev.* **1997**, *26*, 355–364. (c) Ward, M. W. *Chem. Soc. Rev.* **1997**, *26*, 365–375.

(12) (a) BalzaniV.; Scandola, F. *Supramolecular Chemistry*; Ellis Horwood: New York, 1991. (b) Schlicke, B.; De Cola, L.; Belser, P.; Balzani, V. *Coord. Chem. Rev.* **2000**, *208*, 267–275. (c) De Silva, A. P.; Gunaratne, H. Q. N.; Gunnlaugsson, T.; Huxley, A. J. M.; Mccoy, C. P.; Rademacher, J. T.; Rice, T. E. *Adv. Supramol. Chem.* **1997**, *4*, 1–53. (d) Ashton, P. R.; Ballardini, R.; Balzani, V.; Credi, A.; Dress, K. R.; Ishow, E.; Kleverlaan, C. J.; Kocian, O.; Preece, J. A.; Spencer, N.; Stoddart, J. F.; Venturi, M.; Wenger, S. *Chem.−Eur. J.* **2000**, *6*, 3558–3574.

(13) (a) *Supramolecular Chemistry*; Atwood, J. L., Davies, J. E. D., MacNicol, D. D., Vögtle, F., Reinhoudt, D. N., Eds.; Pergamon: Oxford, 1996; Vol. 10, pp 171−185. (b) Bell, T. W.; Hext, N. M. *Chem. Soc. Rev.* **2004**, *33*, 589–598. (c) Sun, S.-S.; Lees, A. J. *Coord. Chem. Rev.* **2002**, *230*, 171–192. (d) de Silva, A. P.; Gunaratne, H. Q. N.; Gunnlaugsson, T.; Huxley, A. J. M.; McCoy, C. P.; Rademacher, J. T.; Rice, T. E. *Chem. Rev.* **1997**, *97*, 1515–1566. (e) Lehn, J. M. *Front. Supramol. Org. Chem. Photochem.* **1991**, *1*, 28. (f) Verhoeven, J. W. *J. Photochem. Photobiol. C* **2006**, *7*, 40–60.

(14) (a) *Phthalocyanine Materials: Structure, Synthesis and Function*, McKeown, N. B., Ed.; Cambridge University Press: Cambridge, 1998. (b) *Phthalocyanine: Properties and Applications*; Leznoff, C. C., Lever, A. B. P., Eds.; VCH: New York, 1993. (c) *The Porphyrin Handbook*; Kadish, K. M., Smith, K. M., Guilard, R., Eds.; Academic Press: San Diego, CA 2003; Vols. *15−20*. (d) de la Torre, G.; Claessens, C. G.; Torres, T. *Chem. Commun.* **2007**, 2000–2015. (e) Kobayashi, N. *Coord. Chem. Rev.* **2002**, *227*, 129–152. (f) Claessens, C. G.; González-Rodríguez, D.; Torres, T. *Chem. Rev.* **2002**, *102*, 835. (g) de la Torre, G.; Vázquez, P.; Agulló-López, F.; Torres, T. *J. Mater. Chem.* **1988**, *8*, 1671.

(15) (a) Linssen, T. G.; Durr, K.; Hanack, M.; Hirsch, A. *J. Chem. Soc., Chem. Commun.* **1995**, *103*, 104. (b) Sastre, A.; Gouloumis, A.; Vázquez, P.; Torres, T.; Doan, V.; Schwartz, B. J.; Wudl, F.; Echegoyen, L.; Rivera, J. *Org. Lett.* **1999**, *1*, 1807–1810. (c) Martìnez-Dìaz, M. V.; Fender, N. S.; Rodrìguez-Morgade, M. S.; Gòmez-López, M.; Diederich, F.; Echegoyen, L.; Stoddart, J. F.; Torres, T. *J. Mater. Chem.* **2002**, *12*, 2095–2099. (d) Guldi, D. M.; Ramey, J.; Martìnez-Dìaz, M. V.; de la Escosura, A.; Torres, T.; Da Ros, T.; Prato, M. *Chem. Commun.* **2002**, 2774–2775.

(16) (a) Gouloumis, A.; Liu, S.-G.; Sastre, A.; Vázquez, P.; Echegoyen, L.; Torres, T. *Chem.−Eur. J.* **2000**, *6*, 3600–3607. (b) Guldi, D. M.; Gouloumis, A.; Vázquez, P.; Torres, T. *Chem. Commun.* **2002**, 2056–2057. (c) Loi, M. A.; Neugebauer, H.; Denk, P.; Brabec, C. J.; Sariciftci, N. S.; Gouloumis, A.; Vázquez, P.; Torres, T. *J. Mater. Chem.* **2003**, *13*, 700–704. (d) Guldi, D. M.; Zilbermann, I.; Gouloumis, A.; Vázquez, P.; Torres, T. *J. Phys. Chem. B* **2004**, *108*, 18485–18489.

(17) (a) Li, M. A.; Denk, P.; Hoppe, H.; Neugebauer, H.; Winder, C.; Meissner, D.; Brabec, C.; Sariciftci, N. S.; Gouloumis, A.; Vazquez, P.; Torres, T. *J. Mater. Chem.* **2003**, *13*, 700–704. (b) Guldi, D. M.; Ramey, J.; Martinez-Diaz, M. V.; de la Escosura, A.; Torres, T.; Da Ros, T.; Prato, M. *Chem. Commun.* **2002**, 2774–2775. (c) Kahnt, A.; Guldi, D. M.; de la Escosura, A.; Martinez-Diaz, M. A.; Torres, T. *J. Mater. Chem* **2008**, *18*, 77–82.

(18) (a) Quintiliani, M.; Kahnt, A.; Vazquez, P.; Guldi, D. M.; Torres, T. *J. Mater. Chem.* **2008**, *18*, 1542–1546. (b) Bottari, G.; Olea, D.; Gomez-Navarro, C.; Zamora, F.; Gomez-Herrero, J.; Torres, T. *Angew. Chem., Int. Ed.* **2008**, *47*, 2026–2031. (c) De la Escosura, A.; Martinez-Diaz, M. V.; Guldi, D. M.; Torres, T. *J. Am. Chem. Soc.* **2006**, *128*, 4112–4118. (d) Rodríguez-Morgade, M. S.; Torres, T.; Atienza-Castellanos, C.; Guldi, D. M. *J. Am. Chem. Soc.* **2006**, *128*, 15145–15154. (e) Jiménez, A. J.; Spänig, F.; Rodríguez-Morgade, M. S.; Ohkubo, K.; Fukuzumi, S.; Guldi, D. M.; Torres, T. *Org. Lett.* **2007**, *9*, 2481–2484.

(19) (a) Chen, Y.; El-Khouly, M. E.; Sasaki, M.; Araki, Y.; Ito, O. *Org. Lett.* **2005**, *7*, 1613–1616. (b) Isosomppi, M.; Tkachenko, N. V.; Efimov, A.; Vahasalo, H.; Jukola, J.; Vainiotalo, P.; Lemmetyinen, H. *Chem. Phys. Lett.* **2006**, *430*, 36–40. (c) Lehtivuori, H.; Kumpulainen, T.; Efimov, A.; Lemmetyinen, H.; Kira, A.; Imahori, H; Tkachenko, N. *J. Phys. Chem. C* **2008**, *112*, 9896–9902. (d) Vuorinen, T.; Kaunisto, K.; Tkachenko, N. V.; Efimov, A.; Alekseev, A. S.; Hosomizu, K.; Imahori, H.; Lemmetyinen, H. *Langmuir* **2005**, *21*, 5383–5390.

(20) (a) Nyokong, T. *Coord. Chem. Rev.* **2007**, *251*, 1707–1722. (b) Nyokong, T. *Curr. Top. Electrochem.* **2003**, *9*, 197–206. (c) Bedioui, F.; Griveau, S.; Nyokong, T.; Appleby, A. J.; Caro, C. A.; Gulppi, M.; Ochoa, G.; Zagal, J. H. *Phys. Chem. Chem. Phys.* **2007**, *9*, 3383–3396.

(21) (a) Kobayashi, N.; Lever, A. B. P. *J. Am. Chem. Soc.* **1987**, *109*, 7433–7341. (b) Kobayashi, N.; Togashi, M.; Osa, T.; Ishii, K.; Yamauchi, S.; Hino, H. *J. Am. Chem. Soc.* **1996**, *118*, 1073–1085. (c) Sielcken, O. E.; van Tilborg, M. V.; Roks, M. F. M.; Hendriks, R.; Drenth, W.; Nolte, J. M. *J. Am. Chem. Soc.* **1987**, *109*, 4261–6265. (d) Sielcken, O. E.; Schram, J.; Nolte, R. J. M.; Schoonman, J.; Drenth, W. *J. Chem. Soc., Chem. Commun.* **1988**, 108–109. (e) Nikolaitchik, A. V.; Korth, O.; Rodgers, M. A. *J. Phys. Chem. A* **1999**, *103*, 7587–7596. (f) Nikolaitchik, A. V.; Rodgers, M. A. J. *J. Phys. Chem. A* **1999**, *103*, 7597–7605.

(22) For cation induced dimerization of crown ether appended porphyrin analogs, see: (a) Thanabal, V.; Krishnan, V. *J. Am. Chem. Soc.* **1982**, *104*, 3643–3650. (b) Thanabal, V.; Krishnan, V. *Inorg. Chem.* **1982**, *21*, 3606–3613. (c) van Willigen, H.; Chandrashekar, T. K. *J. Am. Chem. Soc.* **1986**, *108*, 709–713. (d) Chandrashekar, T. K.; van Willigen, H.; Ebersole, M. *J. Phys. Chem.* **1985**, *89*, 3453–3459. (e) Chitta, R.; Rogers, L. M.; Wanklyn, A.; Karr, P. A.; Kahol, P. K.; Zandler, M. E.; D'Souza, F. *Inorg. Chem.* **2004**, *43*, 6969–6978.

Scheme 1

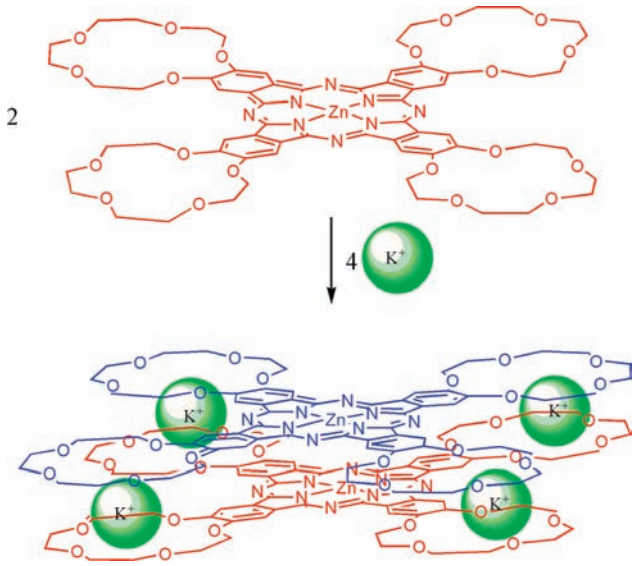

coordinating entity and an alkyl ammonium cation entity as shown in Scheme 2. The pyridine coordinates to the zinc center while the alkyl ammonium ion forms a complex with one of the crown ether entities[10,23] (without destroying the K^+-sandwich dimer) via a "two-point" binding motif[10] (Scheme 2). Utilization of such well-defined multiple modes of binding in a controlled fashion results in the formation of biomimetic supramolecular donor−acceptor conjugate. The photoexcitation of the supramolecular K_4[ZnTCPc]$_2$−fullerene complex affords the charge-separated state with a much longer lifetime as compared with the corresponding zinc porphyrin supramolecular complex.[10] This is clearly demonstrated by time-resolved spectroscopic measurements performed in this study. Thus, the present donor−acceptor building approach using a zinc phthalocyanine dimer provides valuable insight into the importance of special pair dimer not only for efficient charge separation but also for stabilization of the charge-separated states.

Results and Discussion

Steady-State Absorption Studies. Figure 1a shows the UV−vis spectrum of ZnTCPc in benzonitrile, which revealed a Soret-type band at 345 and visible bands at 630 and 676 nm, respectively.[21] Upon addition of K^+, the Soret band revealed a slight increase, while the visible band at 676 nm, often assigned to the monomeric species, completely diminished in intensity with concurrent appearance of a peak at 636 nm, corresponding to the existence of the cofacial dimer[21] as shown in Scheme 1 due to strong exciton coupling.[24] Further, as shown in Figure 1b, a plot of absorbance of the 676 nm band versus the number of equivalents of K^+ added revealed a break at 2, a value expected for the 2:1 stoichiometric ratio between K^+ and ZnTCPc of the K_4[ZnTCPc]$_2$ complex.[25] From the procedure adopted by Thanabal and Krishnan for the determination of the binding constant of related zinc tetrakis(15-crown-5)porphyrin dimer, K_4[ZnTCP]$_2$,[22a] the binding constant for K_4[ZnTCPc]$_2$ formation was found to be $K_{dimer} \approx 5.05 \times 10^{23}$ M^{-5} in benzonitrile. This value is close to that reported for K^+ induced dimer formation ZnTCP,[22a,e] suggesting very stable zinc phthalocyanine dimer formation.

Addition of the functionalized fullerene py$C_{60}NH_3^+$ to K_4[ZnTCPc]$_2$ resulted in a decreased intensity of the 636 nm with the appearance of isosbestic points at 627 and 647 nm (Figure 2a). The Soret band at 345 nm revealed a blue shift of up to 9 nm. A sharp peak at 433 nm corresponding to that of the fulleropyrrolidine was also observed. These spectral shifts are typical of axial coordination of pyridine to zinc phthalocyanine analogs.[26] It should be pointed out here that the addition of fullerene ligands did not cause breaking in the K^+-sandwich dimer since the original zinc phthalocyanine monomer spectrum could not be observed under these conditions. From the data of an independent experiment, a Job's plot was constructed to determine the stoichiometry of the supramolecular complex (Figure 2b) by monitoring the absorbance at 636 nm. Such a plot revealed a break at ~0.63 for the number of moles of py$C_{60}NH_3^+$ to the total number of moles of py$C_{60}NH_3^+$ and K_4[ZnTCPc]$_2$ indicating a 2:1 supramolecular stoichiometry for the fullerene:ZnPc dimer, which is in agreement with the supramolecular structure of tetrad K_4[ZnTCPc]$_2$:(py$C_{60}NH_3^+$)$_2$, shown in Scheme 2. Additionally, the monomeric ZnTCPc-PyC60NH_3^+ dyad, formed by treating 1:1 equivalents of the donor and acceptor, was treated with K^+ ions to check whether the penta coordinated ZnTCPc would form the K^+ induced phthalocyanine dimer. Such an experiment indeed revealed the final spectrum of the tetrad similar to that shown in Figure 2a indicating formation of K^+ induced phthalocyanine dimer of the penta coordinated species, ultimately resulting into the formation of the tetrad. That is, existence of the ZnTCPc dimer and not higher ZnTCPc oligomers under the present experimental conditions is clear from these studies.

The binding constant calculated by constructing the Benesi−Hildebrand plot[27] was found to be $K_{complex} = (2.5 \pm 0.5) \times 10^3$ M^{-1}, suggesting moderate stability for the supramolecular donor−acceptor conjugate (Figure 2c). The observed isosbestic points for K_4[ZnTCPc]$_2$ dimer binding to py$C_{60}NH_3^+$ (Figure 2a) and the straight line Benesi−Hildebrand plot (Figure 2c) suggest occurrence of a one-step binding process for the 1:2 dimer−fullerene complex, that is, simultaneous binding of 2 equiv of py$C_{60}NH_3^+$ to the metal centers of K_4[ZnTCPc]$_2$. In the control experiments, monomeric ZnTCPc was titrated with py$C_{60}NH_3^+$, which also revealed spectral changes characteristic of axial coordination and 1:1 molecular

(23) (a) D'Souza, F.; Chitta, R.; Gadde, S.; Zandler, M. E.; Sandanayaka, A. S. D.; Araki, Y.; Ito, O. *Chem. Commun.* **2005**, 1279–1281. (b) D'Souza, F.; Chitta, R.; Gadde, S.; Zandler, M. E.; McCarty, A. L.; Sandanayaka, A. S. D.; Araki, Y.; Ito, O. *Chem.—Eur. J.* **2005**, *11*, 4416–4428.

(24) (a) Kasha, M. *Radiat. Res.* **1963**, *20*, 55–70. (b) Gouterman, M.; Holten, D.; Lieberman, E. *Chem. Phys.* **1977**, *25*, 139–153. (c) Hunter, C. A.; Sanders, J. K. M.; Stone, A. J. *Chem. Phys.* **1989**, *133*, 395–404. (d) Tran-Thi, T. H.; Lipskier, J. F.; Maillard, P.; Momenteau, M.; Lopez-Castillo, J.-M.; Jay-Gerin, J.-P. *J. Phys. Chem.* **1992**, *96*, 1073–1082. (e) Tran-Thi, T.-H. *Coord. Chem. Rev.* **1997**, *160*, 53–91. (f) Toupance, T.; Ahsen, V.; Simon, J. *J. Am. Chem. Soc.* **1994**, *116*, 5352–5361. (g) Toupance, T.; Benoit, H.; Sarazin, D.; Simon, J. *J. Am. Chem. Soc.* **1997**, *119*, 9191–9197.

(25) A small deviation from the straight line segment around 1 equiv of K^+ is observed in Figure 6b, suggesting 2 equiv of K^+ essentially starts forming the ZnTCPc dimer. Steady-state fluorescence emission data analysis in Figure 6 inset also revealed such a trend.

(26) (a) El-Khouly, M. E.; Rogers, L. M.; Zandler, M. E.; Gadde, S.; Fujitsuka, M.; Ito, O.; D'Souza, F. *ChemPhysChem* **2003**, *4*, 474–481. (b) El-Khouly, M. E.; Araki, Y.; Ito, O.; Gadde, S.; Zandler, M. E.; D'Souza, F. *J. Porphyrins Phthalocyanines* **2006**, *10*, 1156–1164.

(27) Benesi, H. A.; Hildebrand, J. H. *J. Am. Chem. Soc.* **1949**, *71*, 2703–2707.

Scheme 2

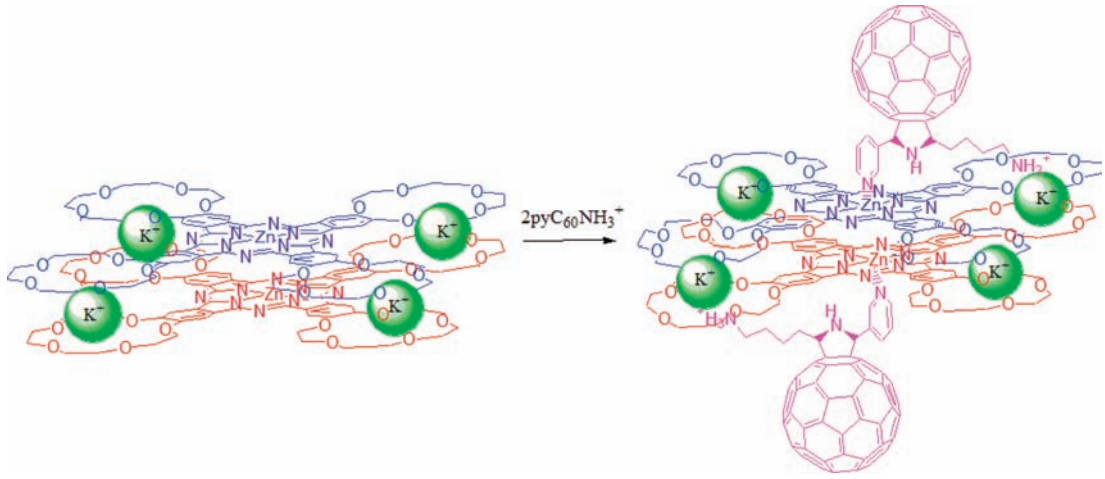

stoichiometry as arrived from Job's plot. The binding constant calculated from the Benesi−Hildebrand plot[27] was found to be $(1.5 \pm 0.05) \times 10^4$ M^{-1}.

DFT B3LYP/3-21G(*) Computational Studies. Various spectroscopic methods including optical absorption and EPR have reported K^+-induced dimerization of crown ether appended phthalocyanines and porphyrins.[22] From the resulting ground state triplet spectrum of the paramagnetic Cu^{2+}-containing porphyrin derivatives, it has been possible to spectroscopically estimate the metal−metal distance of ∼4.1 Å in the dimer.[21,22] In the present study, using the DFT B3LYP/3-21G(*) method,[28] the geometry and electronic structure of the dimer was probed to arrive at the geometry and electronic structures.[29] Figure 3a,b shows the optimized structure of the dimer in two orientations. In the dimer structure, the two phthalocyanine rings are cofacially stacked with a Zn−Zn distance of 3.94 Å and interring N−N distance of 3.97 Å. The N−Zn−Zn−N dihedral angle was found to be less than 1° indicating almost perfect cofacial arrangement, in agreement with spectral shifts shown in Figure 1. The calculated HOMOs and LUMOs for the K^+-induced dimer were all π-orbitals and were nearly degenerate. As predicted for the closely interacting π-systems,[20] the orbital coefficients were localized over both of the phthalocyanine rings (Figure 3c,d). No orbital coefficient was present on the K^+-bound crown ether entities, suggesting absence of their involvement either an electron donor or an electron acceptor in electron transfer reaction.

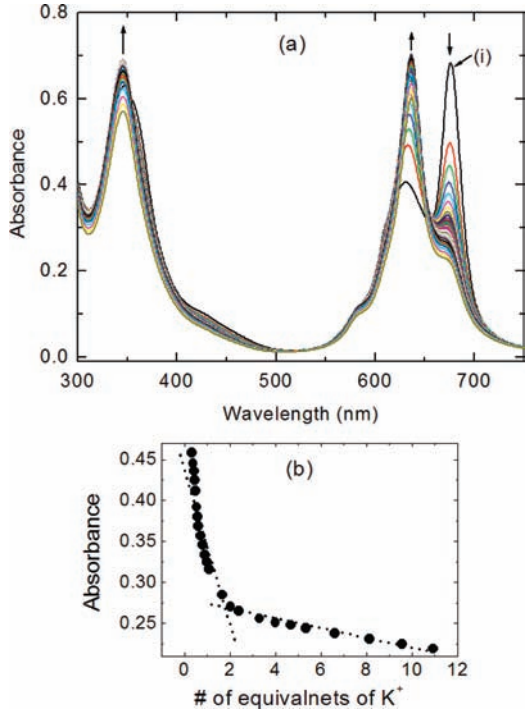

Figure 1. (a) UV−vis spectrum revealing the formation of the cofacial dimer of ZnTCPc (5.0 μM) upon increasing addition of K^+ in benzonitrile. Curve i represents the spectrum of monomeric ZnTCPc in the absence of added K^+. Potassium tetrakis(4-chlorophenyl)borate was used as K^+ source. (b) Plot of absorbance of the 676 nm band versus number of equivalents of K^+ added to arrive at the K^+:ZnTCPc stoichiometry. A break at 2 represents $K_4[ZnTCPc]_2$ formation.

Upon axial coordination of 2 equiv of $pyC_{60}NH_3^+$ to the zinc phthalocyanine dimer, the resulting structures of the conjugate revealed the existence of the $K_4[ZnTCPc]_2$ dimer and formation of new Zn←N coordinate (← represents coordinate bond) and crown ether-NH_3^+ bonds (Figure 4). The center-to-center distance between zinc to the center of C_{60}, R_{CC} was estimated to be ∼10.4 Å, while the edge-to-edge distance, $R_{Ed\text{-}Ed}$ was found to be ∼7.5 Å. As envisioned, the adopted two-point binding strategy involving axial coordination and alkyl ammonium-crown ether binding resulted in complexes of defined distance and orientation.

Electrochemical Studies. Electrochemical studies using cyclic voltammetric technique were performed to evaluate the redox potentials and also to probe the integrity of the supramolecular complex. As shown in Figure 5, the cyclic voltammograms of the monomer ZnTCPc revealed the first oxidation and the first reduction processes located at $E_{1/2} = -0.08$ and $E_{pc} = -1.80$ V vs Fc/Fc^+, respectively (curve i). Upon forming the dimer $K_4[ZnTCPc]_2$ by the addition of K^+ to the solution of ZnTCPc, the oxidation peaks revealed splitting as a consequence of strongly interacting phthalocyanine macrocycles.[22e,30] The split oxidation processes were located at $E_{1/2} = -0.20$ and 0.05 V, respectively, while the reduction peak was located at $E_{pc} = -1.71$ V vs Fc/Fc^+ (curve ii). Addition of 2 equiv of $pyC_{60}NH_3^+$

(28) *Gaussian 03*; Frisch, M. J., et al. Gaussian, Inc.: Pittsburgh, PA, 2003. The full reference is given in Supporting Information.
(29) For applications of DFT on tetrapyrrole-fullerene systems, see: Zandler, M. E.; D'Souza, F. In *DFT Calculations on Fullerenes and Carbon Nanotubes*; Basiuk, V. A., Irle, S., Eds.; Research Signpost: Kerala, India, 2008; pp 81−126.

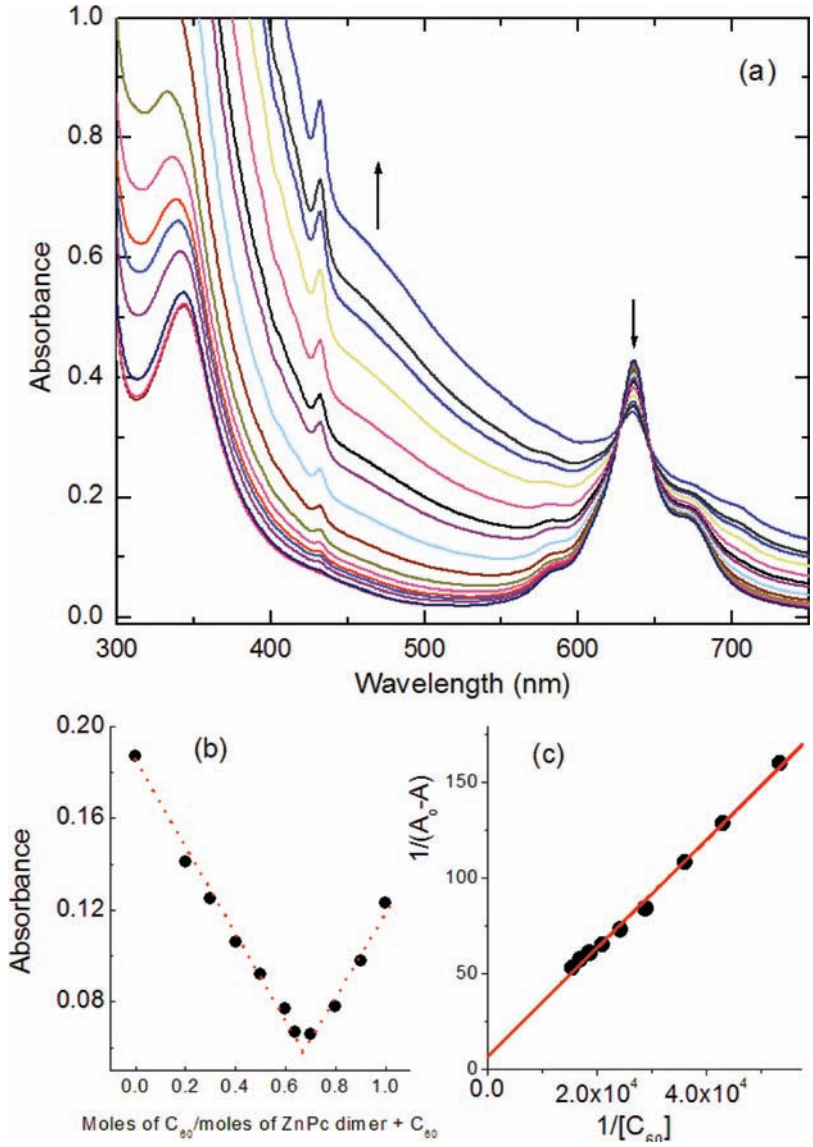

Figure 2. (a) Spectral changes observed during the titration of $pyC_{60}NH_3^+$ to the solution of $K_4[ZnTCPc]_2$ in benzonitrile. (b) Job's plot constructed to obtain the stoichiometry of the supramolecular complex (the absorbance was monitored at 636 nm). (c) Benesi−Hildebrand plot constructed to evaluate the binding constant. A_0 and A represent the absorbance of the ZnPc dimer in the absence and presence of added fulleropyrrolidine, respectively.

(to form the tetrad as shown in Scheme 2) to the $K_4[ZnTCPc]_2$ dimer solution revealed additional changes in the peak potentials; however, the split oxidation peaks, signature for the existence of the dimer in solution, were still retained (curve iii). The potentials of the split oxidation processes were located at $E_{1/2} = -0.18$ and 0.02 V, while the reduction was located at $E_{pc} = -1.62$ V. In addition to this, peaks at $E_{1/2} = -1.02$ and -1.41 V vs Fc/Fc^+ corresponding to the reduction of $pyC_{60}NH_3^+$ were also observed. The lower currents observed for $K_4[ZnTCPc]_2$:$(pyC_{60}NH_3^+)_2$ are due to solution dilution. These results demonstrate the existence of the supramolecular donor−acceptor conjugate, $K_4[ZnTCPc]_2$:$(pyC_{60}NH_3^+)_2$, as depicted in Scheme 2.

The free-energy changes[31] for charge separation ($-\Delta G_{CS}$) via $K_4{}^1[ZnTCPc]_2$* and charge recombination ($-\Delta G_{CR}$) calculated from the electrochemical redox and emission data of ($E_{0-0} = 1.83$ eV for $K_4[ZnTCPc]_2$) were found to be -1.00 and -0.83 eV, respectively, for the supramolecular tetrad. In these calculations the electrostatic term was neglected since the positive and negative charges in the charge-separated state are highly delocalized over the donor and acceptor macrocycles. The magnitude of $-\Delta G_{CS}$ suggests the charge separation process to be located in the lower half of the normal Marcus curve.[32] Interestingly, the magnitude of $-\Delta G_{CR}$ suggests it to be in the upper half of the inverted Marcus curve.[32] That is, lower values of k_{CR} and relatively faster k_{CS} are expected from the free-energy calculations. However, as discussed in the subsequent section,

(30) (a) Shultz, D. A.; Lee, H.; Kumar, R. K.; Gwaltney, K. P. *J. Org. Chem.* **1999**, *64*, 9124–9136. (b) Le Mest, Y.; L'Her, M.; Hendricks, N. H.; Kim, K.; Collman, J. P. *Inorg. Chem.* **1992**, *31*, 835–847. (c) Wasielewski, M. R.; Smith, U. H.; Cope, B. T.; Katz, J. J. *J. Am. Chem. Soc.* **1977**, *99*, 4172–4173. (d) Tanaka, M.; Ohkubo, K.; Gros, C. P.; Guilard, R.; Fukuzumi, S. *J. Am. Chem. Soc.* **2006**, *128*, 14625–14633.

(31) (a) Rehm, D.; Weller, A. *Isr. J. Chem.* **1970**, *7*, 259–271. (b) Mataga, N.; Miyasaka, H. In *Electron Transfer*; Jortner, J., Bixon, M., Eds.; John Wiley & Sons: New York, 1999; Part 2, pp 431−496.

(32) (a) Marcus, R. A.; Sutin, N. *Biochim. Biophys. Acta* **1985**, *811*, 265–322. (b) Marcus, R. A. *Angew. Chem., Int. Ed. Engl.* **1993**, *32*, 1111–1121.

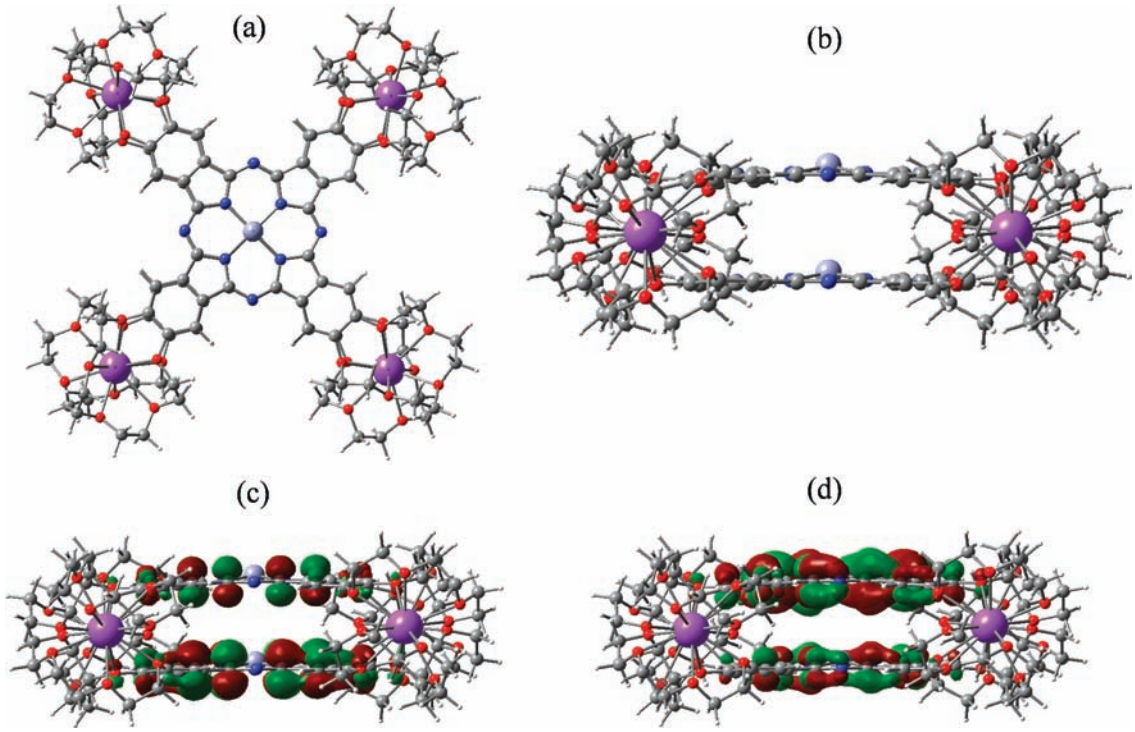

Figure 3. B3LYP/3-21G(*) optimized structure of $K_4[ZnTCPc]_2$ dimer (a and b). The HOMO and LUMO of the dimer are shown in panels c and d, respectively.

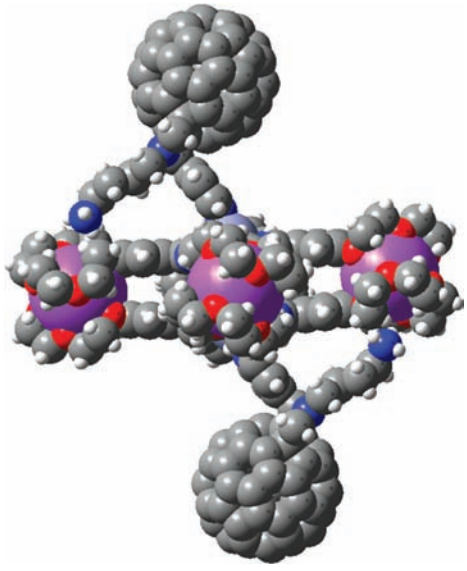

Figure 4. B3LYP/3-21G(*) optimized structure of the supramolecular $K_4[ZnTCPc]_2$:$(pyC_{60}NH_3^+)_2$ conjugate. The counter cations and anions are omitted to keep the structures simple.

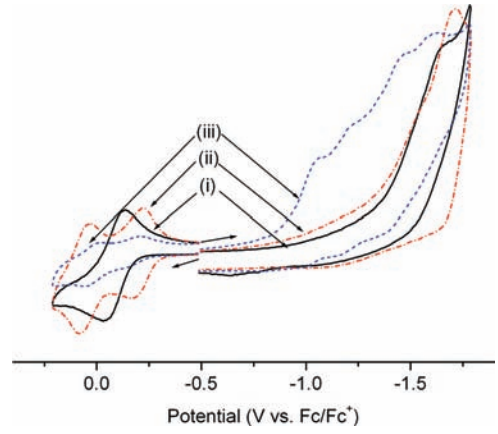

Figure 5. Cyclic voltammograms of (i) ZnTCPc, (ii) $K_4[ZnTCPc]_2$, and (iii) $K_4[ZnTCPc]_2$:$(pyC_{60}NH_3^+)_2$ obtained by the addition of 2 equiv of $pyC_{60}NH_3^+$ in benzonitrile, 0.1 M $(n\text{-}C_4H_9)_4NClO_4$. Scan rate = 100 mV/s. The concentration of porphyrins was ~0.1 mM, and the potassium tetrakis(4-chlorophenylborate) used to induce dimerization was ~5 mM.

the k_{CR} might further slow down due to rigidity of the phthalocyanine macrocycle, which is expected to lower the reorganization energy.

Steady-State and Time-Resolved Emission Studies. Steady-state fluorescence spectrum of ZnTCPc showed two emission bands in benzonitrile located at 684 and 753 nm, respectively. In agreement with the earlier reports,[21e,f] addition of K^+ leading into the formation of the dimer $K_4[ZnTCPc]_2$, the fluorescence of zinc phthalocyanine was quenched over 90% of its original intensity as a consequence of static quenching (Figure 6). Further, as shown in the inset of Figure 6, a plot of emission intensity of the 684 nm band versus the number of equivalents of K^+ revealed a break at 2, a value expected for the 2:1 stoichiometric ratio between K^+ and ZnTCPc of the $K_4[ZnTCPc]_2$ complex,[25] in agreement with the earlier discussed absorbance data (Figure 1). It may also be mentioned here that the addition of size appropriate Na^+ for 15-crown-5 entities, leading into the formation of $Na_4[ZnTCPc]$ monomer, caused no significant changes in the emission behavior, that is, no fluorescence quenching was observed. Further, addition of $pyC_{60}NH_3^+$ to the dimer solution to form the supramolecular donor−acceptor complex caused additional quenching of the already quenched $K_4[ZnTCPc]_2$ emission to over 98%, suggesting occurrence of additional photochemical events in the supramolecular complex.

Time-Resolved Emission Studies. Figure 7 shows emission decay profiles of ZnTCPc under different solution conditions.

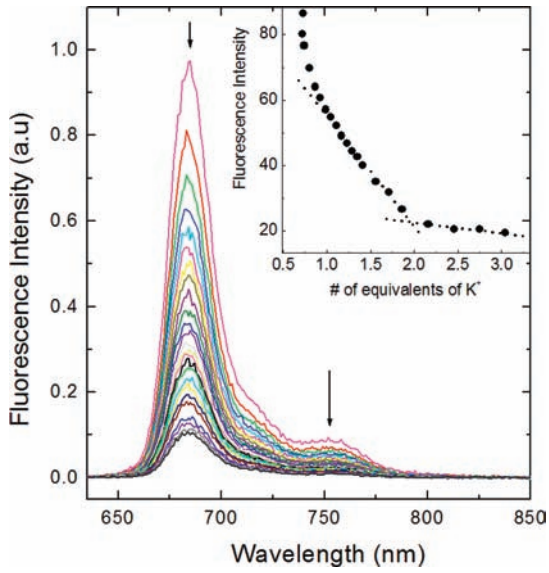

Figure 6. Effect of K^+ addition on the fluorescence emission of ZnTCPc (5 μM) in benzonitrile. λ_{ex} = 610 nm. Potassium tetrakis(4-chlorophenyl)borate (0.1 equiv each addition) was used as K^+ source. Figure inset shows a plot of emission intensity of the 684 nm band versus number of equivalents of K^+ added to arrive at the K^+:ZnTCPc stoichiometry. A break at 2 represents K_4[ZnTCPc]$_2$ formation.

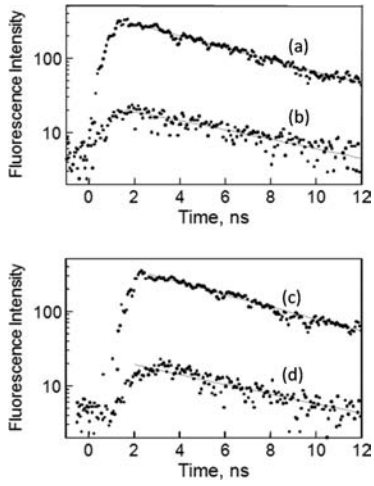

Figure 7. Time-resolved fluorescence spectrum of (a) ZnTCPc, (b) K_4[ZnTCPc]$_2$ formed by the addition of K^+ to ZnTCPc (1:4 equiv), (c) ZnTCPc + $pyC_{60}NH_3^+$ (1:1 equiv), and (d) tetrad K_4[ZnTCPc]$_2$:$(pyC_{60}NH_3^+)_2$ in benzonitrile. The excitation wavelength was 410 nm, and the decay was monitored at 687 nm. Potassium tetrakis(4-chlorophenyl)borate was used as K^+ source.

The tetra crown substituted ZnTCPc revealed monoexponential decay with a lifetime of 5.2 ns, close to that reported for zinc phthalocyanines in the literature.[21e,f] The dimer K_4[ZnTCPc]$_2$ formed by the addition of K^+ also revealed a monoexponential decay with a lifetime of 7.4 ns, which was almost similar to that of ZnTCPc (Figures 7a and b). The slight increase in lifetime could be attributed to the deaggregation of the zinc phthalocyanine upon addition of K^+. This observation supports the static quenching observed under steady state conditions shown in Figure 6. Surprisingly, the ZnTCPc:$pyC_{60}NH_3^+$ formed by mixing 1:1 equivalents of the monomer ZnTCPc and $pyC_{60}NH_3^+$ and the tetrad K_4[ZnTCPc]$_2$:$(pyC_{60}NH_3^+)_2$ also revealed monoexponential decays with lifetimes of 5.0 and 6.9 ns, respectively (Figure 7c,d). These results suggest absence of any photoinduced processes originating from the singlet excited state of ZnTCPc. To confirm such a process, further femtosecond transient absorption studies were performed, as discussed below.

Femtosecond Transient Absorption Spectral Studies. The absence of photoinduced electron transfer from the singlet excited state of both monomeric and dimeric forms of ZnTCPc in the presence of bound fullerene was confirmed from these studies. As shown in Figure 8a for ZnTCPc, the transient features were that of the excited singlet state undergoing intersystem crossing within 190 ps (Figure 8d).[33] The transient features observed for the dimer K_4[ZnTCPc]$_2$ were not significantly different. The transient observed at 564 nm decayed within 210 ps (Figure 8e). Interestingly, the tetrad K_4[ZnTCPc]$_2$:$(pyC_{60}NH_3^+)_2$ had a significantly faster decay component of 34 ps (41%) and a slow decay component of 200 ps (59%) as shown in Figure 8f. The lifetime of the slow component is the same as that of K_4[ZnTCPc]$_2$. Thus, the fast component corresponds to the quenching of the singlet excited state of K_4[ZnTCPc]$_2$ by $pyC_{60}NH_3^+$ in the tetrad K_4[ZnTCPc]$_2$:$(pyC_{60}NH_3^+)_2$. This is supported by the agreement of the percentage of the fast component (41%) with the percentage of the tetrad formation (41%) estimated from the $K_{complex}$ value $(2.7 \pm 0.6) \times 10^3$ M^{-1} under the experimental conditions in Figure 8f where the concentration of $pyC_{60}NH_3^+$ is 2.6×10^{-4} M. A similar observation was made for the dyad ZnTCPc:$pyC_{60}NH_3^+$.

A careful examination of the spectral data in Figure 8c clearly shows absence of transient bands corresponding to either the $ZnPc^{+\bullet}$ around 860 nm or $C_{60}^{\bullet-}$ around 1000 nm within the allowed time scale of 3000 ps of our instrument. These results suggest occurrence of a much slower electron transfer process, if any, as predicted by the free-energy calculations, perhaps originating from the triplet excited state of ZnTCPc. To confirm this and identify the electron transfer products, transient absorption studies using nanosecond laser flash photolysis have been performed.

Nanosecond Transient Absorption Spectral Studies. The confirmation of the charge-separated (CS) state and the role of phthalocyanine dimer in stabilizing the CS state were evident from these studies. As shown in Figure 9a, the transient absorption spectra of the dyad ZnTCPc:$pyC_{60}NH_3^+$, formed by complexing equimolar $pyC_{60}NH_3^+$ and ZnTCPc in the absence of K^+, revealed bands at 870 and 1000 nm corresponding to the formation of $ZnTCPc^{\bullet+}$ and $C_{60}^{\bullet-}$, respectively.[15−18] Additional bands around 500 and 700 nm were also observed corresponding to the triplet excited state of fullerene entity ($^3C_{60}$*).[15] The decay time profile of the absorption at 500 and 700 nm due to $^3C_{60}$* is clearly different from the decay of the absorption at 870 and 1000 nm due to the CS state, and the lifetime agrees with that of $^3C_{60}$*. Thus, the transient absorption at 500 and 700 nm is assigned to the triplet excited state of unbound $pyC_{60}NH_3^+$. The quantum yields of charge-separated state are determined as 0.50 ± 0.08 for ZnTCPc:$pyC_{60}NH_3^+$ and 0.29 ± 0.06 for K_4[ZnTCPc]$_2$:$(pyC_{60}NH_3^+)_2$ from the absorption of fulleropyrrolidine anion at 1000 nm (ε_{1000} = 4700 M^{-1} cm^{-1}),[34] using the absorbance of the triplet−triplet absorption of free base tetraphenylporphyrin, ε_{690} = 3500 M^{-1} cm^{-1},

(33) Howe, L.; Zhang, J. Z. *J. Phys. Chem. A* **1997**, *101*, 3207–3213.
(34) (a) Imahori, H.; Tamaki, K.; Guldi, D. M.; Luo, C.; Fujitsuka, M.; Ito, O.; Sakata, Y.; Fukuzumi, S. *J. Am. Chem. Soc.* **2001**, *123*, 2607–2617. (b) Luo, C.; Fujitsuka, M.; Huang, C.-H.; Ito, O. *Phys. Chem. Chem. Phys.* **1999**, *1*, 2923–2928.
(35) (a) Pekkarinen, L.; Linschitz, H. *J. Am. Chem. Soc.* **1960**, *82*, 2407–2411. (b) Gratz, H.; Penzkofer, A. *Chem. Phys.* **2000**, *254*, 363–374.

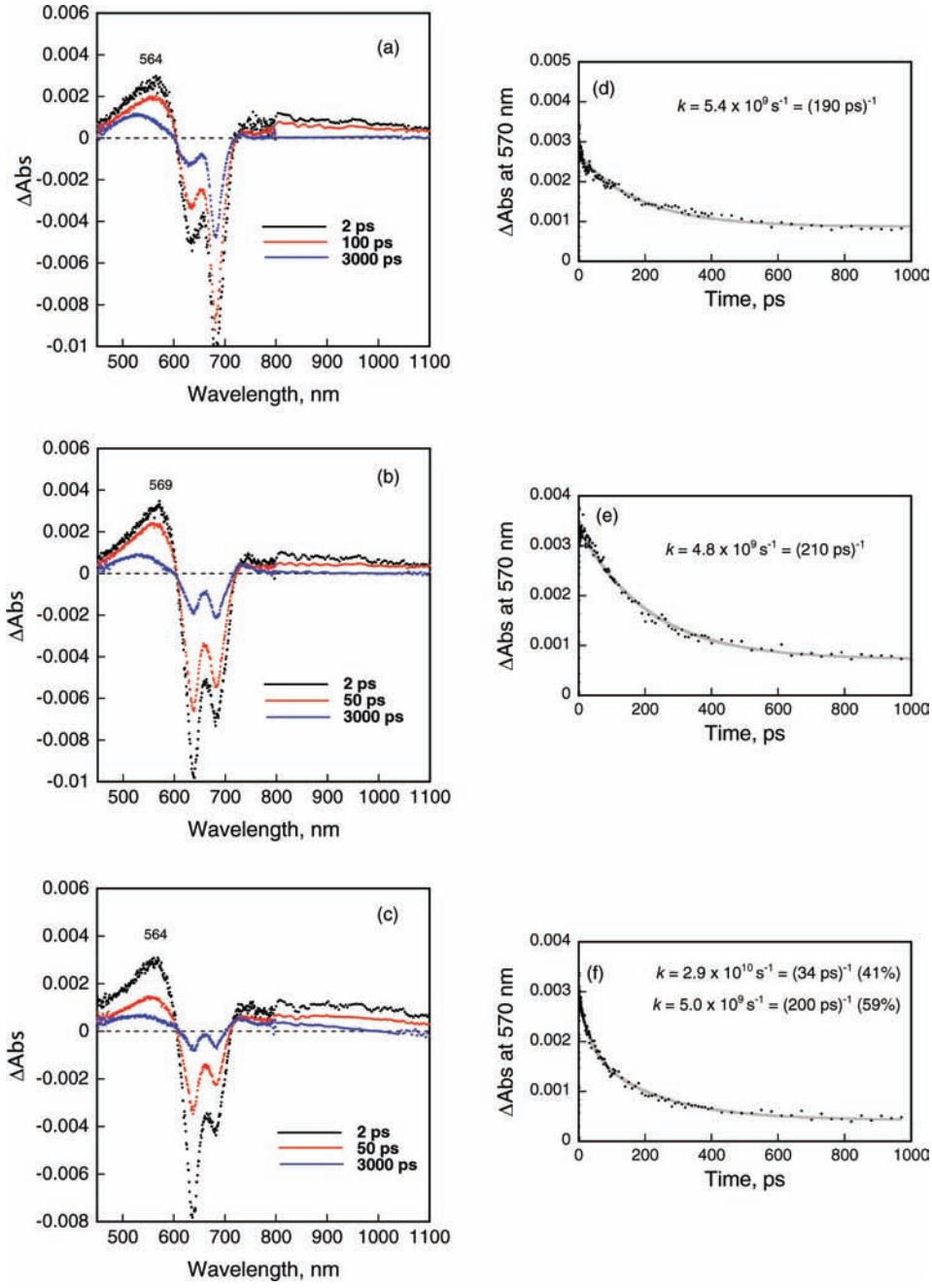

Figure 8. Femtosecond transient absorption spectrum recorded at different time intervals for (a) ZnTCPc (2.5×10^{-4} M), (b) ZnTCPc + K^+ to form the cofacial dimer K_4[ZnTCPc]$_2$, and (c) tetrad K_4[ZnTCPc]$_2$:(p$yC_{60}NH_3^+$)$_2$ (1.3×10^{-4} M) constructed by mixing ZnTCPc with 2 equiv of K^+ and 1 equiv of p$yC_{60}NH_3^+$ in benzonitrile. $\lambda_{ex} = 410$ nm. Panels d−f at the right show the first-order decay monitored at 570 nm.

as a reference.[35] These quantum yields agree within experimental errors with the percentages of ZnTCPc:p$yC_{60}NH_3^+$ (56 ± 5%) and K_4[ZnTCPc]$_2$:(p$yC_{60}NH_3^+$)$_2$ (21 ± 4%) estimated from the formation constants (1.25×10^4 and 2.7×10^3 M^{-1}, respectively) under the experimental conditions in Figure 9 where the concentration of p$yC_{60}NH_3^+$ is 1.0×10^{-4} M. Unfortunately, the concentration of p$yC_{60}NH_3^+$ for the nanosecond laser flash photolysis measurements is limited as a result of the absorbance at the excitation wavelength, precluding higher quantum yields.

The decay of the absorption at 870 and 1000 nm due to the CS state obeys first-order kinetics. This indicates that the charge recombination occurs in the supramolecular complex. The rate constant of charge recombination, k_{CR} obtained by monitoring the decay of $C_{60}^{\bullet-}$ was found to be 2.1×10^5 s^{-1}, which resulted in a lifetime of 4.8 μs for the CS state. Upon forming the supramolecular tetrad, that is, coordination of 2 equiv of p$yC_{60}NH_3^+$ to K_4(ZnTCPc)$_2$, the transient spectral features were almost similar to that observed for the dyad. That is, diagnostic bands corresponding to the formation of $ZnTCPc^{+\bullet}$ and $C_{60}^{\bullet-}$ were observed at the expected wavelengths (Figure 9b). The calculated k_{CR} was found to be 1.5×10^5 s^{-1}, resulting into a lifetime of 6.7 μs for the CS state. This lifetime is significantly longer than the value (50 ns) reported for the corresponding tetrad using a zinc porphyrin dimer.[10] Such drastically increased lifetime of the CS state in the phthalocyanine dimer-C_{60} supramolecular complex, K_4[ZnTCPc]$_2$:(p$yC_{60}NH_3^+$)$_2$, as compared to the corresponding porphyrin dimer complex may result

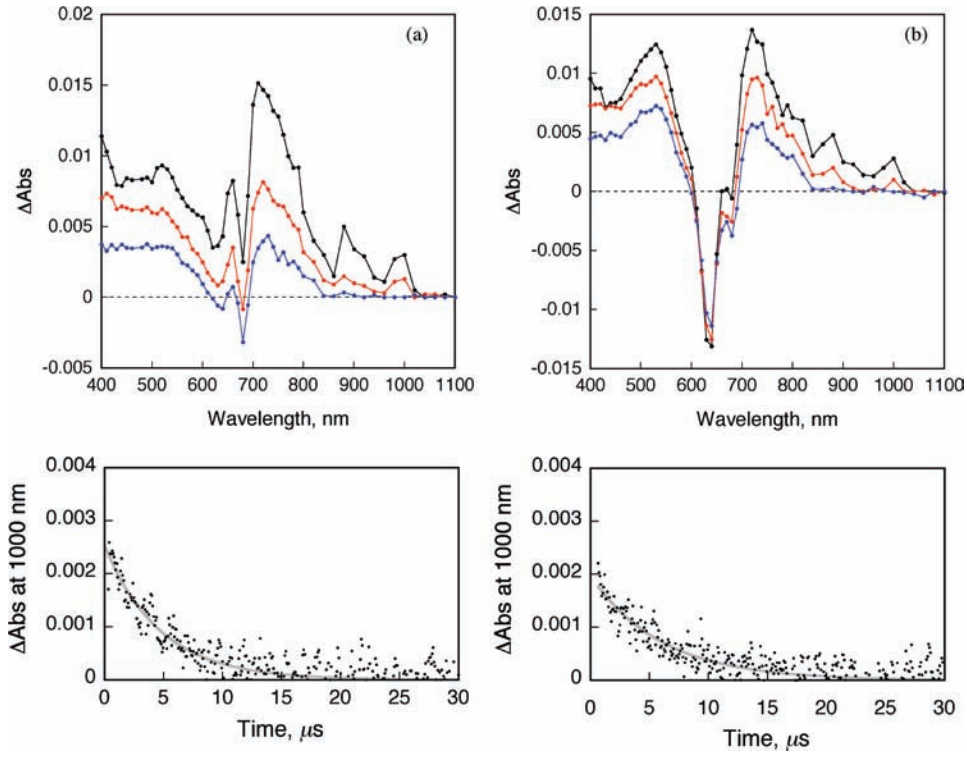

Figure 9. Nanosecond transient absorption spectra of (a) dyad ZnTCPc:py$C_{60}NH_3^+$ (1.0×10^{-4} M) formed by mixing equimolar ZnTCPc and py$C_{60}NH_3^+$ and (b) tetrad K_4[ZnTCPc]$_2$:(py$C_{60}NH_3^+$)$_2$ (5.0×10^{-5} M) observed by 430 nm laser irradiation at 1, 4, and 10 μs time intervals in benzonitrile. The lower panel shows time profiles of fullerene anion radical peak at 1000 nm. The first-order decay is fitted by the solid line.

from a smaller reorganization energy of electron transfer for the more π-expanded phthalocyanine macrocycle relative to the porphyrin macrocycle.[36] Such a small reorganization energy of electron transfer also results in the much slower charge separation from the singlet excited state (^{1}ZnTCPc*) as compared to the intersystem crossing to afford the triplet excited state (^{3}ZnTcPc*), as discussed below.

The energy diagram of the dyad (ZnTCPc:py$C_{60}NH_3^+$) and the tetrad (K_4[ZnTCPc]$_2$:(py$C_{60}NH_3^+$)$_2$) is shown in Figure 10, where the ZnPc and C_{60} denote the zinc phthalocyanine and fullerene moieties, respectively. Upon photoexcitation of the supramolecular complex, the singlet excited state (^{1}ZnPc*) is formed, which undergoes the intersystem crossing to afford the triplet excited state (^{3}ZnPc*-C_{60}) as shown in Figure 8.[37] The driving force of charge separation (0.89 and 1.00 eV for the dyad and tetrad, respectively) is significantly larger than the reorganization energy of electron transfer judging from the reorganization energy of electron transfer of the porphyrin supramolecular complex (0.54 eV).[38] In such a case, the charge separation from ^{1}ZnPc* is deeply in the Marcus inverted region,[32] where the CS rate is too slow to compete with the intersystem crossing. Then, the CS state is formed via electron

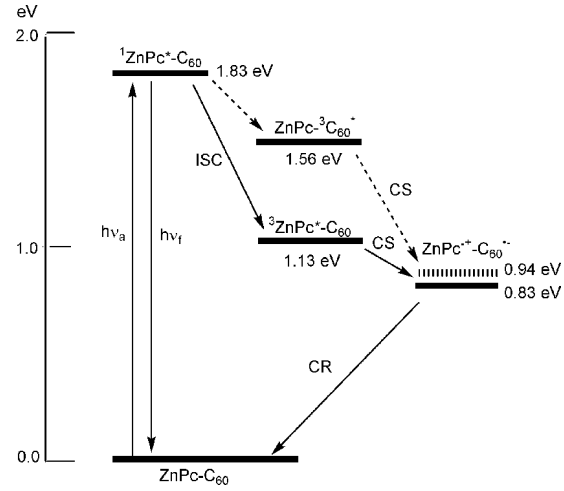

Figure 10. Energy level diagram showing the different photochemical events in the present supramolecular cofacial phthalocyanine dimer-fullerene conjugate (abbreviated as ZnPc-C_{60} for simplicity). The dotted line represents the energy level of the CS state of the monomeric phthalocyanine-fullerene dyad.

transfer from ^{3}ZnPc* as shown in Figure 9.[39] Unfortunately the CS rate from ^{3}ZnPc* was too slow to be determined by femtosecond laser flash photolysis but too fast to be determined by nanosecond laser flash photolysis. The CS time scale is

(36) For the favorable effects of π-expansion of porhyrins on electron-transfer reactions, see: (a) Fukuzumi, S.; Ohkubo, K.; E, W.; Ou, Z.; Shao, J.; Kadish, K. M.; Hutchison, J. A.; Ghiggino, K. P.; Sintic, P. J.; Crossley, M. J. *J. Am. Chem. Soc.* **2003**, *125*, 14984–14985. (b) Ohkubo, K.; Sintic, P. J.; Tkachenko, N. V.; Lemmetyinen, H.; Ou, Z.; Shao, J.; Kadish, K. M.; Crossley, M. J.; Fukuzumi, S. *Chem. Phys.* **2006**, *326*, 3–14. (c) Kadish, K. M.; Wenbo, E.; Sintic, P. J.; Ou, Z.; Shao, J.; Ohkubo, K.; Fukuzumi, S.; Govenlock, L. J.; McDonald, J. A.; Try, A. C.; Cai, Z.-L.; Reimers, J. R.; Crossley, M. J. *J. Phys. Chem. B* **2007**, *111*, 8762–8774. (d) Fukuzumi, S.; Ohkubo, K.; Zhu, W.; Sintic, M.; Khoury, T.; Sintic, P. J.; Wenbo, E.; Ou, Z.; Crossley, M. J.; Kadish, K. M. *J. Am. Chem. Soc.* **2008**, *130*, 9451–9458.

(37) The photoexcitation of the supramolecular complex with $\lambda = 430$ nm also results in formation of $^1C_{60}$*. However, the contribution of $^1C_{60}$* is negligible because no $^3C_{60}$* is detected, as shown in Figure 8c.

(38) Tanaka, M.; Ohkubo, K.; Gros, C. P.; Guilard, R.; Fukuzumi, S. *J. Am. Chem. Soc.* **2006**, *128*, 14625–14633.

(39) Vincett, P. S.; Voigt, E. M.; Rieckoff, K. E. *J. Chem. Phys.* **1971**, *55*, 4131–4140.

roughly estimated to be in the range of 3−100 ns. As a result of the small reorganization energy of the relatively rigid phthalocyanine macrocycle in addition to that of fullerene,[40] long-lived CS states were attained as shown in Figure 9. The longer CS lifetime of the phthalocyanine dimer-C_{60} supramolecular complex, $K_4[ZnTCPc]_2$:$(pyC_{60}NH_3^+)_2$ (6.7 μs), as compared to that of the monomer complex, ZnTCPc:$pyC_{60}NH_3^+$ (4.8 μs), despite the smaller driving force of electron transfer in the Marcus inverted region may result from the smaller reorganization energy of electron transfer of the phthalocyanine dimer (0.83 eV) compared to that of the monomer (0.94 eV). The long CS lifetime with the driving force of 0.83 and 0.94 eV is consistent with no observation of the CS process from ^{1}ZnPc* with the driving force of 0.89 and 1.00 eV, when the ISC process is much faster than the CS process.

Conclusions

An outstanding supramolecular tetrad as a photosynthetic reaction center mimic of "special pair" dimer self-assembled to electron acceptors has been assembled using zinc phthalocyanine as electron donor and fullerene as electron acceptor. This methodology, fully based on well-defined self-assembly methods without utilization of covalent bonding to link the different entities, resulted into the formation of discrete supramolecular donor−acceptor conjugate. The structure of this supramolecule was deduced from spectroscopic, computational, and electrochemical methods. On the basis of detailed analysis of the kinetic data from the time-resolved emission and transient absorption spectroscopy of different time scales, it was found that the charge separation occurs from the triplet excited state of the ZnPc moiety to the C_{60} moiety rather than the singlet excited state to afford the long-lived CS state of the supramolecular complex. The longer CS lifetime of the phthalocyanine dimer-C_{60} supramolecular complex, $K_4[ZnTCPc]_2$:$(pyC_{60}NH_3^+)_2$ (6.7 μs), has been attained as compared to that of the monomer complex, ZnTCPc:$pyC_{60}NH_3^+$ (4.8 μs), despite the smaller driving force of back electron transfer because of smaller reorganization energy of the phthalocyanine dimer, clearly delineating the role of the cofacial phthalocyanine dimer in stabilizing the CS state in donor−acceptor systems.

Experimental Section

Chemicals. Buckminsterfullerene, C_{60} (+99.95%), was from SES Research, (Houston, TX). All reagents were from Aldrich Chemicals (Milwaukee, WI), and the bulk solvents utilized in the syntheses were from Fischer Chemicals. The syntheses of $pyC_{60}NH_3^+$ [23] and crown ether appended phthalocyanines[21a] were carried out according to literature methods with some modifications.

Synthesis of 4,5-Dibromobenzo-15-crown-5. In a two neck 500 mL round-bottomed flask, benzo-15-crown-5 (2.2 g, 8.19 mmol), iron powder (64.1 mg, 1.147 mmol), and a catalytic amount of I_2 (100 mg) were added to 100 mL of dry CH_2Cl_2, and 0.90 L (0.0175 mol) of Br_2 was added to above reaction mixture at 0 °C over a period of 2 h. The reaction mixture was stirred for 16 h at room temperature, filtered, and poured into 100 mL of 10% aqueous NaOH. The organic layer was separated, washed with water, dried, and removed under vacuum. The crude compound was recrystallized using hexane to obtain the dibromo product. The yield was 93.2%. ^{1}H NMR in $CDCl_3$: δ (ppm) 7.04 (s, 2H, phenyl-H), 3.75−4.20 (m, 16H, crown -CH_2-).

Synthesis of 4,5-Dicyanobenzo-15-crown-5. 4,5-Dibromobenzo-15-crown-5 (2.97 g, 6.99 mmol), CuCN (1.90 g, 21.33 mmol), and pyridine (332 μL, 4.09 mmol) were dissolved in 100 mL of dry DMF. Then the reaction mixture was refluxed for 20 h under dry nitrogen. The mixture was cooled, poured into 200 mL of 25% ammonium hydroxide, and extracted with $CHCl_3$. The organic layer was washed with water, dried, and concentrated. The crude compound was purified on neutral alumina column using hexane/$CHCl_3$ (50:50 v/v) as eluent. Yield: 552 mg (37.2%).^{1}H NMR in $CDCl_3$: δ (ppm) 7.14 (s, 2H, phenyl-H), 3.75−4.30 (m, 16H, crown -CH_2-).

Synthesis of 4,5-Isoiminoindolen-benzo-15-crown-5. Dicyano product (500 mg, 1.57 mmol) was dissolved in 200 mL of dry methanol. A suspension of dry sodium methoxide (168 mg, 3.10 mmol) was added to the reaction mixture under argon atmosphere. Then, anhydrous ammonia was bubbled through the reaction mixture for 8 h with refluxing. The solvent was evaporated under reduced pressure, and the crude product (450 mg) was used for next step without purification.

Synthesis of 4,5,4′,5′,4″,5″,4‴,5‴-Tetrakis(1,4,7,10,13-pentaoxatrideca-methylene)phthalocyanine (H_2TCPc). A precursor of isoiminoindoline compound (450 mg) was dissolved in dry 2-(dimethylamino)ethanol (5.0 mL) under argon atmosphere. The reaction mixture was heated and stirred at 150 °C for 44 h in an oil bath. After solvent evaporation, the resulting dark green reaction mixture was purified on neutral alumina column using $CHCl_3$/MeOH (95:5 v/v) as eluent. Yield: 55 mg. ^{1}H NMR in $CDCl_3$: δ (ppm) 8.00 (m, 8H, phthalocyanine-H), 3.50−4.75 (m, 64H, crown -CH_2-), −3.40 (s, 2H, inner H of Pc). UV/vis ($CHCl_3$): λ_{max} = 346, 421, 601, 645, 662, 701 nm.

Synthesis of Zinc 4,5,4′,5′,4″,5″,4‴,5‴-Tetrakis(1,4,7,10,13-pentaoxatrideca-methylene)phthalocyanine (ZnTCPc). H_2TCPc and a large excess of zinc acetate were dissolved in ethanol, and the reaction mixture was refluxed for several hours in the dark, until the 4-band Q spectrum of H_2TCPc had disappeared. Then, the organic layer was washed with water, dried, and evaporated under reduced pressure. The crude product was purified on neutral alumina column using chloroform as eluent. Yield: 50 mg (87%). ^{1}H NMR in $CDCl_3$: δ (ppm) 8.00 (m, 8H, phthalocyanine-H), 3.50−4.75 (m, 64H, crown-CH_2−). UV/vis ($CHCl_3$): λ_{max} = 350, 421, 610, 677 nm.

Synthesis of 2-(3′-Pyridyl)-5-(n-butylammonium)-3,4-fulleropyrrolidine. H-Lys-(Boc)-OH (100 mg, 0.406 mmol) and 3-pyridine carboxyaldehyde (76 mL) were added to a solution of C_{60} (100 mg, 0.138 mmol) in toluene, and the mixture was refluxed for 3 h. The solvent was evaporated by vacuum, followed by purification on silica gel by using toluene/ethyl acetate 8:2 to obtain the *N*-Boc-protected compound (85 mg, 62%). Next, to a dichloromethane solution of the N-Boc-protected compound (75 mg in 5 mL) were added trifluoroacetic acid (3 mL) and *m*-cresol (50 mL), and the mixture was stirred for 3 h. The solvent and acid were removed under vacuum, and the solid product (66 mg, 97%) was washed in toluene several times to desired product. ^{1}H NMR in $CDCl_3$: δ (ppm) 9.13, 8.60, 8.48, 7.64 (s, d, t, t, 4H, 3 pyridine H), 6.15, 5.17, 5.14 (s, d, d, 3H, pyrrolidine H), 3.01−1.94 (d, m, m, m, 8H, -$(CH_2)_4$-). UV/vis (MeOH): λ_{max} = 204, 254.5 nm.

Instrumentation. ^{1}H NMR spectra were obtained from chloroform-d_1 solutions using a Varian 400 MHz NMR spectrometer with tetramethylsilane as internal standard. The UV−vis spectral measurements were carried out with a Shimadzu Model 1600 UV−vis spectrophotometer. The fluorescence emission was monitored by using a Varian Eclipse spectrometer. Cyclic voltammograms were recorded on a EG&G PARSTAT electrochemical analyzer using a three electrode system. A platinum button electrode was used as the working electrode. A platinum wire served as the counter electrode and an Ag/AgCl electrode was used as the reference. Ferrocene/ferrocenium redox (Fc/Fc^+) couple was used as an internal standard. All solutions were purged prior to electrochemical and spectral measurements using argon gas.

(40) (a) Imahori, H.; Yamada, H.; Guldi, D. M.; Endo, Y.; Shimomura, A.; Kundu, S.; Yamada, K.; Tadashi Okada, T.; Sakata, Y.; Fukuzumi, S. *Angew. Chem., Int. Ed.* **2002**, *41*, 2344–2347. (b) Fukuzumi, S.; Ohkubo, K.; Imahori, H.; Guldi, D. M. *Chem.—Eur. J.* **2003**, *9*, 1585–1593.

The computational calculations were performed by DFT B3LYP/3-21G(*) methods with GAUSSIAN 03 software package[31] on high speed computers. The frontier orbitals were generated using the GaussView program.

Time-Resolved Fluorescence Absorption Measurements. Femtosecond fluorescence upconversion measurements were carried out using a Clark-MXR 2010 laser system and an optical detection system provided by Ultrafast Systems (Halcyone). The source for the excitation and gate pulses were derived from the fundamental output of Clark laser system (775 nm, 1 mJ/pulse and fwhm = 150 fs) at a repetition rate of 1 kHz. The instrument involves the frequency mixing of incoherent fluorescence (resulting from exciting a sample with a short laser pulse) with a probe laser pulse (fwhm = 150 fs) in a nonlinear optical crystal. The setup of optical description is designed to work with a regeneratively amplified Ti-sapphire laser. The gate beam is sent through a computer-controlled optical delay stage and is focused on the nonlinear crystal together with the fluorescence from the sample. The excitation pulse (λ = 410 nm) is sent through a half-wave plate/neutral density assembly and is focused on the sample. The excitation of the sample can be performed in transmissive (for clear samples) or reflective modes (for opaque samples). The resulting fluorescence is collected by an objective and together with a gate beam is sent to a nonlinear crystal. The upconverted fluorescence signal is collected after the crystal with an objective and sent through the set of filters and a monochromator for spectral purification. The PMT and the single photon counting unit are used to monitor the signal intensity.

Subpicosecond time-resolved fluorescence decays were measured by a Photon Technology International GL-3300 with a Photon Technology International GL-302 and a nitrogen laser/pumped dye laser system equipped with a four-channel digital delay/pulse generator (Standard Research System Inc. DG535) and a motor driver (Photon Technology International MD-5020). The excitation wavelength was 525 nm with use of Coumarin 540A (Exciton Co, Ltd.).

Time-Resolved Transient Absorption Measurements. Femtosecond laser flash photolysis was conducted using a Clark-MXR 2010 laser system and an optical detection system provided by Ultrafast Systems (Helios). The source for the pump and probe pulses were derived from the fundamental output of Clark laser system (775 nm, 1 mJ/pulse and fwhm = 150 fs) at a repetition rate of 1 kHz. A second harmonic generator introduced in the path of the laser beam provided 410 nm laser pulses for excitation. Nearly 95% of the fundamental output of the laser was used to generate the second harmonic, while 5% of the deflected output was used for white light generation. Prior to generating the probe continuum, the laser pulse was fed to a delay line that provided an experimental time window of 1.6 ns with a maximum step resolution of 7 fs. The pump beam was attenuated at 5 μJ/pulse with a spot size of 2 mm diameter at the sample cell where it was merged with the white probe pulse in a close angle (<10°). The probe beam after passing through the 2 mm sample cell was focused on a 200 μm fiber optic cable that was connected to a CCD spectrograph (Ocean Optics, S2000-UV-vis for visible region and Horiba, CP-140 for NIR region) for recording the time-resolved spectra (450−800 and 800−1400 nm). Typically, 5000 excitation pulses were averaged to obtain the transient spectrum at a set delay time. The kinetic traces at appropriate wavelengths were assembled from the time-resolved spectral data.

Nanosecond time-resolved transient absorption measurements were carried out using the laser system provided by UNISOKU Co., Ltd. Measurements of nanosecond transient absorption spectrum were performed according to the following procedure. A deaerated solution containing a dyad was excited by a Panther OPO pumped by Nd:YAG laser (Continuum, SLII-10, 4−6 ns fwhm) at λ = 430 nm. The photodynamics was monitored by continuous exposure to a xenon lamp (150 W) as a probe light and a photomultiplier tube (Hamamatsu 2949) as a detector. Transient spectra were recorded using fresh solutions in each laser excitation. The solution was deoxygenated by argon purging for 15 min prior to measurements.

Acknowledgment. This work is supported by the National Science Foundation (CHE 0804015 to F.D.), a Grant-in-Aid (nos. 19205019 and 19750034 to S.F. and K.O.), KOSEF/MEST through WCU project (R31-2008-000-10010-0), and a Global COE program, "the Global Education and Research Center for Bio-Environmental Chemistry" from the Ministry of Education, Culture, Sports, Science and Technology, Japan.

Supporting Information Available: Complete citation details of ref.[28] This material is available free of charge via the Internet at http://pubs.acs.org.

JA903467W